1993

The effects of compaction on inclination of the Pigeon Point formation, California

Jodie M. Davi
Lehigh University

AUTHOR:

Davi, Jodie M.

TITLE:

The Effects of Compaction on Inclination of the Pigeon Point Formation, California

DATE: January 16, 1994

THE EFFECTS OF COMPACTION ON INCLINATION OF THE PIGEON POINT FORMATION, CALIFORNIA

by

Jodie M. Davi

A Thesis

Presented to the Graduate Committee

of Lehigh University

in Candidacy for the Degree of

Master of Science

in

Geological Sciences

Lehigh University

1993

This thesis is accepted and approved in partial fulfillment of the requirements for the degree of Master of Science.

12/16/93
(date)

Advisor

Chair of Department

Acknowledgements

I would like to thank my advisor, Dr. Ken Kodama, my god-like mentor, for his support, high expectations and unending enthusiasm for this project. Dr. Robert Butler (University of Arizona) and Dr. Duane Champion (U.S.G.S. Menlo Park) generously provided samples and many helpful comments. I gratefully acknowledge Dr. Carl Moses for providing moral support, laboratory equipment, and many hours of helpful discussion. The experimental work would not have been possible without the help (and presence) of George and Scott. Laurie and Nancy provided many of hours of help, shoulders to lean on, and outrageous lunches. I would like to thank Andrew and Maria for many thought-provoking discussions and painfully honest questions. I need to thank Laurie and Ed for providing sound advice, moral support, nutritionally balanced meals and a home-away-from-home. Dr. Joyce Castro encouraged me to start this project, and I thank her. Lastly, I would like to thank Jeffrey, who kept me going when I didn't think I could. This work was supported by NSF grant OCE-8911306.

Table of Contents

List of Figures

List of Tables

Abstract

This project is a combination of two studies: The first is a paleomagnetic, rock magnetic and compaction study of the Cretaceous Pigeon Point Formation from northern California which was conducted to determine whether its anomalously shallow inclinations *(Champion et al., 1984)* are due either to 2500 km of northward displacement or compaction shallowing. The second is a test of the *Jackson et al. (1991)* model for correcting inclination shallowing using two sets of samples from New Mexico's Nacimiento Formation and Argentina's Corral Quemado Formation. The Nacimiento Formation has a known inclination shallowing of 8°, while the Corral Quemado Formation shows no inclination shallowing.

Champion et al's (1984) four sites from the Pigeon Point Formation (at the Pigeon Pt. locality) were augmented by collecting an additional three sites. Detailed alternating field demagnetization isolated a characteristic remanence at these three sites. The mean of the site means of the combined data set yields a direction (I=43.4°, D=349.0°, α_{95}=10.2°), which is 23.1° shallower than the expected Cretaceous direction. Material collected from the Pigeon Point Formation was disaggregated by sonification, given a PDRM with I=60° and compacted in six separate experiments up to maximum pressures of 0.13 MPa with volume losses of over 50%. Inclination shallowing of 12°-20° was observed only after alternating-field demagnetization to 100 mT. When the inclination shallowing is plotted versus the samples' AAR, it lies on the theoretical curve for magnetic particles with a particle anisotropy a=4/3 (*Jackson et al.,* 1991).

The AAR fabric of the collected Pigeon Point samples show a composite fabric due to compaction and turbidite deposition. A lineated fabric resulted from the turbidity flow, and a foliated fabric resulted from compaction. These two fabrics are end-members of magnetic grain distribution and correcting for each fabric gives

bounds to our inclination shallowing correction. These bounds range from a mean paleomagnetic direction of D= 351.6°, I= 53.1° with $\alpha 95$= 11.3° for a lineated fabric, and D= 349.4°, I= 50.4° with $\alpha 95$= 10.4° for a foliated fabric. This suggests that about one-half of the observed inclination shallowing of the Pigeon Point Formation can be explained by compaction/turbidite deposition effects.

The known inclinations and inclination errors of the Nacimiento and Corral Quemado Formations were plotted against measured anisotropy of anhysteretic remanence (AAR). This plot shows a large scatter in both data sets. The results from the Nacimiento and Corral Quemado Formations show there are factors other than particle anisotropy that affect inclination shallowing, as the model by *Jackson et al. (1991)* assumes.

Introduction

The debate about the importance of compaction-caused inclination shallowing in sedimentary rocks has been intensified recently by new developments in California tectonics. Anomalous paleomagnetic directions have been found in both sedimentary and batholithic rocks along the western coast of North America *(Butler et al., 1991)* (Fig. 1). Discordant paleomagnetic directions were initially reported by *Teissere and Beck (1973)* for the Cretaceous Peninsular Ranges batholith. The Peninsular Ranges batholith has a paleomagnetic declination which indicates 25° clockwise rotation about a vertical axis and an inclination which indicates 11° of northward transport with respect to interior North America since Cretaceous time, based on the assumption that paleohorizontal equals present horizontal *(Teissere and Beck, 1973; Hagstrum et al.; 1985; Butler et al., 1991)* (Fig. 2).

Anomalous paleomagnetic directions in Eocene, Paleocene, and Cretaceous marine sedimentary rocks have, to varying degrees, agreed with the anomalous batholithic results. Paleomagnetic inclination of the Tyee and Flournoy turbidites did not show any significant variations with coeval volcanic rocks and this encouraged others to undertake paleomagnetic studies of turbidites *(Champion et al., 1984; Patterson, 1984; Hagstrum et al., 1985)*. Subsequent paleomagnetic investigations of turbidites on the Salinia terrane (*Champion et al., 1984*), Valle Formation *(Patterson, 1984)* and the Baja Peninsula units (*Hagstrum et al., 1985*) all showed a shallow inclination with respect to cratonic directions. *Champion et al. (1984)* reported results from Cretaceous and Paleocene turbidites of the Salinia terrane as indicative of 2500 km of northward transport of Salinia between Late Cretaceous and Eocene time. These results were further supported by *Kanter and Debiche (1985)* and *Kanter (1988)* who confirmed the arrival of Salinia by Eocene time, at the latest. *Patterson (1984)* reported the Upper Cretaceous Valle Formation of Baja California as having

northward transport of 1000 km, inferred from shallow inclinations, while *Hagstrum et al. (1985)* reported Mesozoic units of Baja California as indicative of 11° of post-Cretaceous northward latitudinal transport relative to cratonic North America. The data from *Champion et al. (1984), Patterson (1984),* and *Hagstrum et al. (1985)* all provide evidence for large amounts of northward transport (up to 2500 km).

Butler et al. (1991) however, raise serious questions about large scale transport interpretation. Recent metamorphic and K-Ar work *(Silver et al., 1979; Silver and Chappell, 1988)* indicate that the Peninsular Ranges batholith could have been tilted 21° about a northwest axis (Fig. 2). Removing this tilt would cause the batholith's anomalous direction to come into agreement with the expected cratonic field *(Butler et al., 1991).* This eliminates evidence for shallow inclinations in plutonic rocks and re-opens the possibility of compaction-caused inclination shallowing in sedimentary rocks that show discordant directions since Champion *et al. (1984)* and *Hagstrum et al. (1985)* had ruled out the effects of syndepositional inclination shallowing of Pigeon Point because of the presence of bioturbation. Bioturbation of the sediments suggests post-depositional remanence (pDRM) which has been shown to be accurate *(Verosub, 1977; Kent, 1973; Tucker, 1980; Ellwood, 1984).* Although sediments have been shown to carry an accurate post-depositional remanence (pDRM) *(Irving, 1957; Verosub, 1977)*, the inclination of this signal has been shown to shallow during compaction both in the laboratory *(Blow and Hamilton, 1978; Anson and Kodama, 1987; Deamer and Kodama, 1990; Kodama and Sun, 1992)* and in marine sediments collected from Deep Sea Drilling Project cores *(Arason and Levi, 1990; Tarduno, 1990; Celaya and Clement, 1988).* One model for pDRM compaction shallowing suggests that while the porosity of the sediments is high, the magnetic grains are free to rotate and align themselves to the Earth's field, but when porosity decreases the magnetic grains are 'locked-in' and unable to realign to any changes in the magnetic field. This would suggest that the largest magnetic

grains have experienced the most compaction shallowing *(Irving and Major, 1964; Hamano, 1980)*. Another model suggests inclination shallowing may instead result from adherence of elongate magnetite particles to clay particles *(Anson and Kodama, 1987; Deamer and Kodama, 1990; Kodama and Sun, 1992)*. Once the magnetic particles become attached to the clay particles they are then believed to be rotated towards the bedding plane and follow the development of the clay fabric *(Anson and Kodama, 1987; Deamer and Kodama, 1990)*. This would suggest that the finest magnetic grains would suffer the most inclination shallowing. In either model development of the magnetic fabric is a regular process.

Jackson et al. (1991) have developed a model to correct for compaction-induced inclination shallowing. This model uses the anisotropy of anhysteretic remanence (AAR) to recognize and correct for the effects of compaction on a sediment's inclination. *Jackson et al.'s* model is based on the relationship between depositional remanent magnetization (DRM) intensity and the applied field strength (H):

$$DRM \propto H \tag{1}$$

therefore

$$DRM = ARM * H \tag{2}$$

where anhysteretic remanence magnetization (ARM) is a proportionality constant that applies to both the vertical and horizontal components

$$DRM_{vert} = ARM_{vert}\ H_{vert}$$

$$DRM_{horz} = ARM_{horz}\ H_{horz}$$

Dividing these equations yields

$$\frac{DRM_{vert}}{DRM_{horz}} = \frac{ARM_{vert}\ H_{vert}}{ARM_{horz}\ H_{horz}} \tag{3}$$

Assuming a depositional fabric, which has ARM_{vert} as K_{min} and ARM_{horz} as K_{max}, where K is the anisotropy's eigenvalue, equation (3) becomes

$$\tan I_{DRM} = \frac{K_{min}}{K_{max}} * \tan I_H \quad (4)$$

which can be rearranged:

$$\frac{K_{min}}{K_{max}} = \frac{\tan I_H}{\tan I_{DRM}} \quad (5)$$

where I_{DRM} and I_H are the inclinations of DRM and the applied field, respectively

The measurement of the tensor (K) therefore provides a method for recognizing and correcting for DRM inclination errors *(Jackson et al., 1991).*

Kodama and Sun (1992) have shown through laboratory experiments that *Jackson et al's (1991)* model does not apply to sediments in which magnetic particles were randomized during the early stages of compaction. This randomization can occur naturally through the process of bioturbation and in the early stages of compaction.

Any paleogeographic reconstructions based on the paleomagnetism of sedimentary rocks that do not take into account the effects of compaction may have inaccurate paleolatitudes. The low paleolatitudes of coastal California and Baja California suspect terranes may result from compaction-caused inclination shallowing rather than northward transport *(Butler et al. 1991).* Therefore, the recognition and correction of compaction effects on sedimentary rocks could change the tectonic/paleogeographic interpretation of California.

This project entails two major components. The first, and most significant part involves studying the effects of compaction on the Pigeon Point Formation of western California through standard paleomagnetic measurements, AAR measurement, and laboratory disaggregation and artificial compaction of those sediments. The second part of this study involves an independent test of *Jackson et*

al.'s (1991) theoretical model for correcting compaction-induced inclination shallowing by a rock magnetic study of the Nacimiento and Corral Quemado Formations in New Mexico and Argentina, respectively.

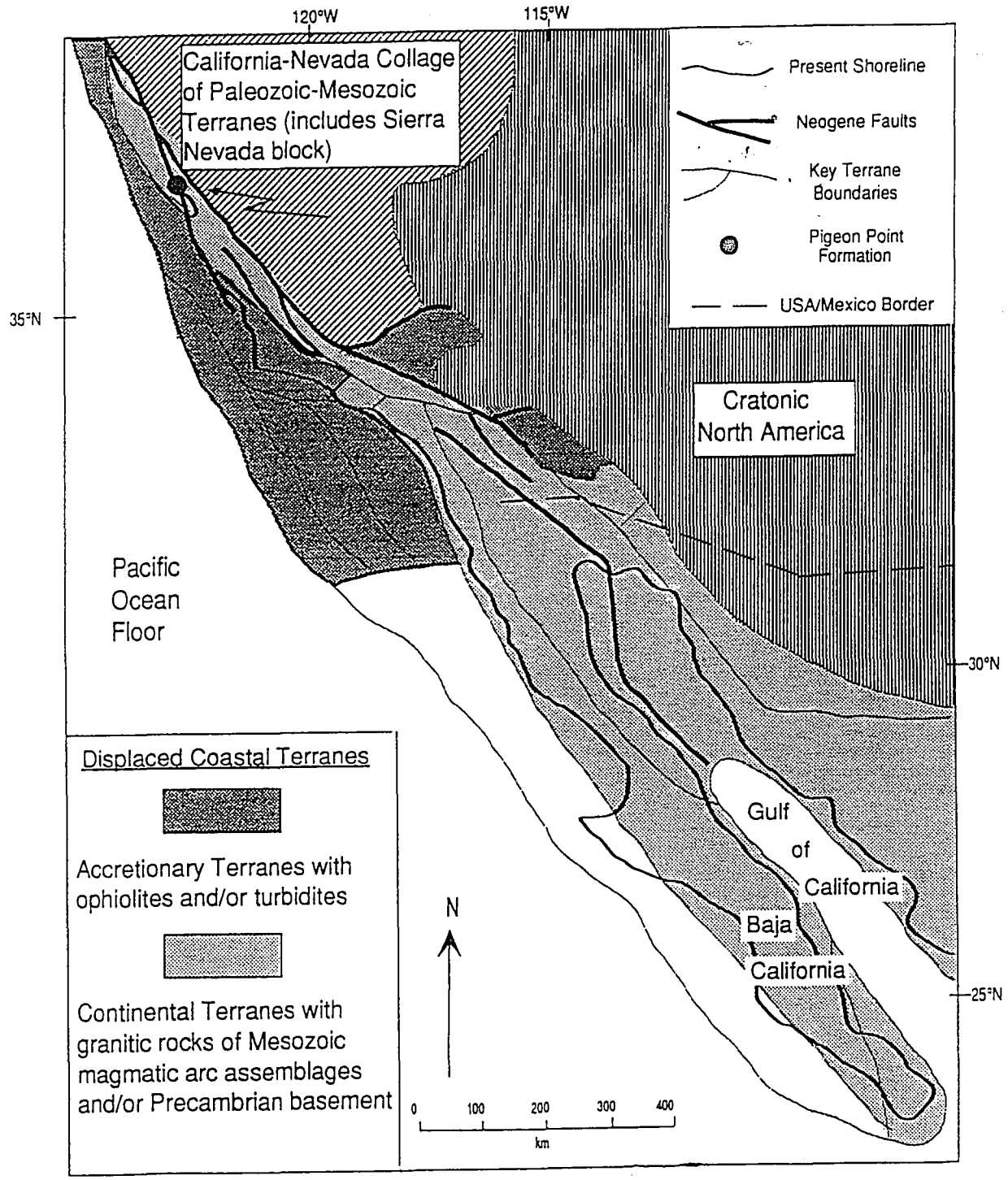

Figure 1
Location of Pigeon Point Formation in relation to terrane boundaries in coastal California, Baja California, and adjacent regions. (From *Butler et al., 1991*)

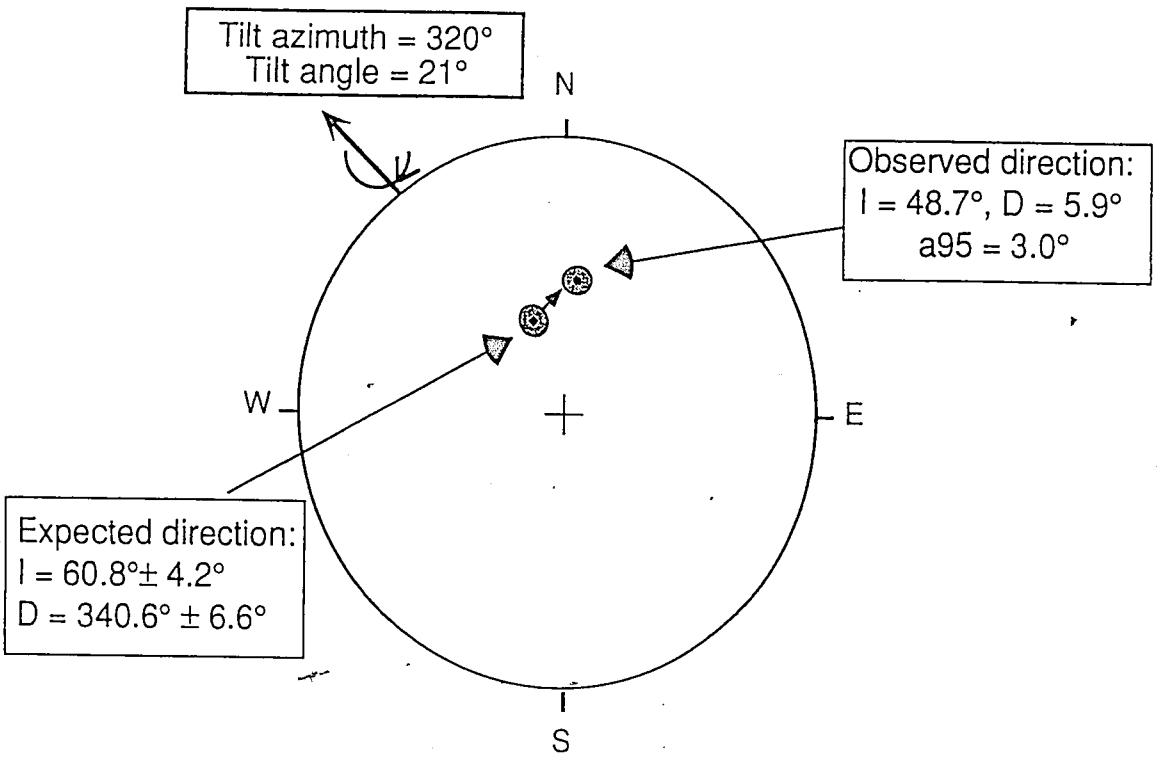

Figure 2
Equal-area projection of observed and expected paleomagnetic direction from the Peninsular Ranges batholith in southern California. Stippled area is 95% confidence limit. Tilt required to deflect expected direction to the observed direction is 21° (±5°) about an axis with azimuth 320° (±10°). (From *Butler et al., 1991*)

Methods

Pigeon Point

The Pigeon Point Formation was chosen for this project because previous studies of the Pigeon Point Formation have been used to support the northward transport of Salinia *(Champion et al., 1984)*. The stratigraphy and sedimentology of the Pigeon Point Formation indicate a progradational depositional sequence with submarine fan to shelf environments *(Howell and Vedder, 1978)*. The lower portion of the sequence is dominated by thick-bedded, coarse to medium-grained turbidites, while the middle section is dominated by layers of fine-grained silt and mud overlain by conglomerates and pebbly mudstone *(Champion et al., 1984)*.

Twenty-nine samples were collected from three sites within the Pigeon Point Formation. The samples were taken from fine-grained layers because the coarse-grained layers frequently showed iron-oxide staining, which can cause overprinting of the original magnetic direction of a sample *(Champion et al., 1984)*. Detailed alternating-field demagnetization was performed on twenty samples, and detailed thermal demagnetization was performed on the remaining nine samples. This small data set was augmented with samples provided by Duane Champion from four sites he had previously collected *(Champion et el., 1984)*. Characteristic magnetizations for each sample were determined using principal component analysis *(Kirschvink, 1980)* of detailed alternating-field demagnetization data provided by Duane Champion. After demagnetization, anisotropy of anhysteretic remanence (AAR) was measured for each rock sample *(McCabe et al., 1985)*, except those samples that were thermally demagnetized. Thermal demagnetization of the Pigeon Point sample resulted in the growth of secondary hematite. Since AAR measures the fabric of the remanence-carrying grains, the fabric would be altered with the introduction of

authigenic hematite and would not reflect the true magnetic fabric of the sedimentary rock.

Hand samples collected from Pigeon Point were disaggregated for compaction experiments using two different techniques: (1) small fragments were placed in an ultrasonic cleaning device or (2) a larger sample was exposed to an ultrasonic probe. These techniques were chosen to preserve the original shape of the rock's sedimentary grains while freeing the magnetic particles from the non-magnetic matrix. Thin sections made of Pigeon Point core samples were compared with smear-slides of the Pigeon Point disaggregated material, to verify that the original grain sizes of the samples were truly being preserved.

The compaction experiment involved making a slurry from the disaggregated material. Slurries were prepared by adding oven dried disaggregated sediments to *instant ocean*, a solution which chemically approximates ocean water. The slurries were prepared for individual experiments to avoid possible evaporation and changes in porosity. The slurry had a water content of 100% and an 80% porosity before compaction, which is equivalent to the porosity and water content of marine sediments at the water-sediment interface *(Nobes, et al., 1986)*. The porosity was determined by the equation

$$\eta = \left[\left(\frac{\rho_g - \rho}{\rho_g - \rho_w}\right)\right] \qquad (6)$$

where $\rho = (W_g + W_w)/(V_b)$

and η is total porosity,

ρ_g is grain density,

ρ is natural bulk density,

ρ_w is water density,

W_g is weight of grains,

W_w is weight of water,

V_b is bulk sample volume.

The grain density was assumed to be 2.6 g/cm^3 based on sample mineralogy determined by X-ray diffraction analysis. The analysis indicated the presence of the clay minerals kaolinite and illite and also quartz, which have grain densities of 2.594 g/cm^3, 2.660 g/cm^3, and 2.600 g/cm^3 respectively.

The slurry was placed in an acrylic cylinder (diameter = 1.5 cm) with a removable bottom plate. A porous stone was used as a plunger to compact the sediments. The samples were compacted with a continuous load applied to the plunger. Water dripping into the tank provided the load (see *Hamano, 1980, Anson and Kodama, 1987, Deamer and Kodama, 1990;* and *Kodama and Sun, 1990* for more details). The time for each compaction experiment varied between 2-8 hours. The total run time is related to the final pressure of the compacted sample (approximately 0.0157 MPa/hr).

Compaction experiments with the disaggregated material were conducted in a known magnetic field ($50° < I < 60°$). This range of inclinations was selected since the expected inclination for the Pigeon Point Formation calculated from the Cretaceous pole for cratonic North America, is 66°. The magnetic field was regulated using two pairs of Helmholtz coils. The samples were given a postdepositional remanence (pDRM) by stirring the sediments and letting them settle in the known magnetic field *(Tucker, 1980).* The magnetic remanence of the slurry was measured before compaction with a two-axis CTF cryogenic magnetometer. The final magnetic direction of the sample was determined by removing the compacted sample from the sample holder and alternating-field demagnetizing the sample.

Volume loss was monitored continuously during compaction. Samples were compacted to final pressures of 0.0314, 0.0471, 0.0628, 0.0785, and 0.1256 MPa (Fig. 3). These pressures were chosen to delineate the break in slope observed by *Deamer*

and Kodama (1990) and *Sun and Kodama (1992)* in the void ratio versus pressure compaction curves.

Once the compaction experiment was completed, AAR of the compacted sample was measured. The inclination and anisotropy data obtained from the compacted samples were then compared with theoretical curves from *Jackson et al. (1991)* which relate AAR anisotropy to the inclination shallowing (Fig. 4). From this comparison, an estimate of the individual magnetic particle anisotropy can be made.

Based on the estimated particle anisotropy, a theoretical curve of inclination shallowing vs. remanence anisotropy, based on the compaction experiments, for the Pigeon Point Formation could be generated using the formula:

$$\frac{1}{f} = \left(\frac{\left(\frac{2}{3} / \left(1 + \frac{1}{\frac{q_x}{q_z}} \right) \right)^{(a+2)} - 1}{\left(\frac{2}{3} / \left(\frac{q_x}{q_z} + 1 \right) \right)^{(a+2)} - 1} \right) \qquad (7)$$

where q_x/q_z is the ratio of the maximum and minimum AAR magnitudes, 1/f is equivalent to $\tan I_O / \tan I_C$, where I_O and I_C are expected and compacted inclinations, respectively, and *a* is the particle anisotropy *(Jackson et al. 1991)*. This curve assumes a slope which is a function of particle anisotropy, *a,* based on a volume loss with one horizontal dimension held constant which results in a triaxial magnetic particle distribution. If we assume volume loss with the horizontal cross-section dimension held constant, the resulting magnetic particle distribution will be oblate. Whereas, if volume loss occurs with the vertical dimension and one horizontal dimension held constant, the resulting magnetic particle distribution would be prolate. Similar theoretical curves were generated assuming sample shapes which are oblate and prolate (See Appendices A, B, and C) (Fig. 5).

Using the theoretical curve generated for the Pigeon Point Formation from the compaction experiments, the following relationship can be used to determine I_o, the original inclination of the rocks:

$$\ln\left(\frac{\tan Io}{\tan Ic}\right) = \ln\left(\frac{1}{f}\right) \qquad (8)$$

where 1/f is derived from equation (7) and qx/qz are AAR ratios.

The variables q_x and q_z are the eigenvalues of the maximum and minimum directions for anisotropy, respectively, and I_c is the compacted inclination *(Jackson et al., 1991).*

Test of Jackson et al.'s (1991) Model

Nacimiento Formation and Corral Quemado Formation

Two sets of samples, obtained from R. F. Butler, serve as an independent test of *Jackson et al.'s (1991)* inclination-shallowing correction technique. The first set are samples collected from the Nacimiento Formation of the San Juan Basin, New Mexico. The Nacimiento Formation consists of a mid-Paleocene, flat-lying sequence of terrestrial sedimentary rocks. The paleomagnetic study by *Butler and Taylor (1978)* indicates a mean direction of magnetization (I = 51.3°, D = 343.9°). When compared to the Paleocene pole for North America, based on work by *Diehl et al. (1983)*, the Nacimiento appears to have an average inclination shallowing of 8° (± 3°).

The second set of samples were collected from the Miocene-Pliocene continental sediments, claystones, siltstones and sandstones of the Catamarca Province in northwestern Argentina. The observed mean direction of magnetization for these samples is I=-46.9°, D=26.6° *(Butler et al., 1984).* The paleomagnetic directions obtained from the Catamarca Province are similar to the axial geocentric dipole direction for South America (I=-45.9°, D=0°) *(Butler et al., 1984).* These

results indicate that there is no inclination error evident since the mean inclination of the sediments agrees with the predicted inclination for South America.

These samples provide an ideal independent test of *Jackson et al.'s (1991)* model. The demagnetized directional data previously collected by *Butler and Taylor (1978)* and *Butler et al. (1984)* combined with AAR measurements, as presented here, provide the necessary information to test *Jackson et al.'s (1991)* theoretical model.

The two sets of samples obtained from R. F. Butler had previously been demagnetized by alternating-field demagnetization. Measurement of AAR was done on all but four samples, two from each set, which had a very strong magnetic intensity and could not be completely demagnetized. These samples had probably been used for IRM acquisition.

Once AAR measurements were completed, Equation (8) could be used and a plot of ln(kmax/kmin) vs. ln(tan Io/tan Ic) could be compared to *Jackson et al.'s (1991)* theoretical curves.

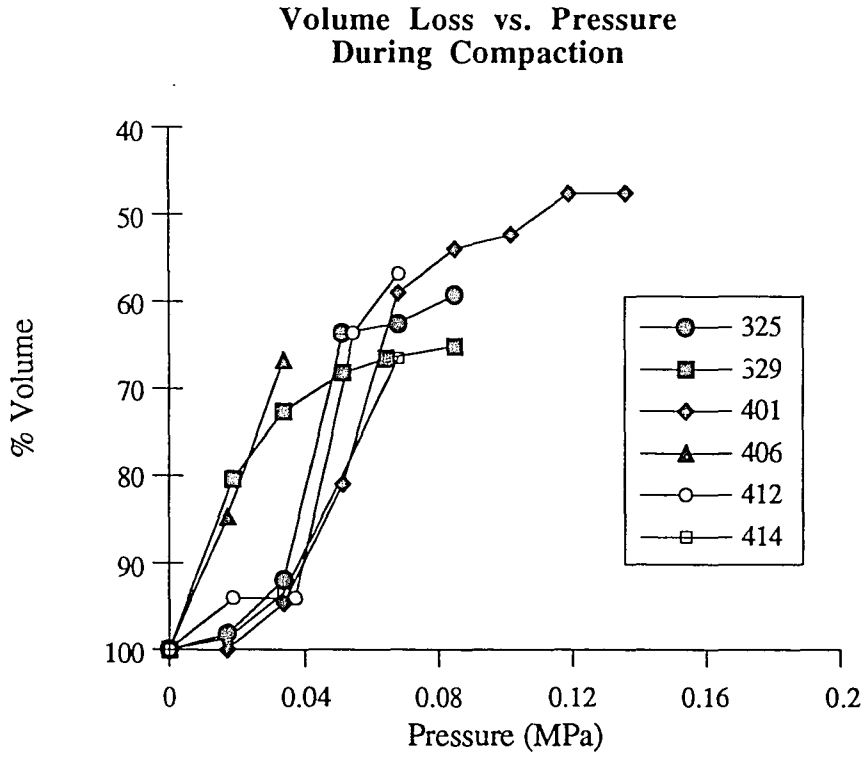

Figure 3
Volume Loss vs. Pressure for the six samples that were compacted. Each sample was plotted to observe the compaction behavior.

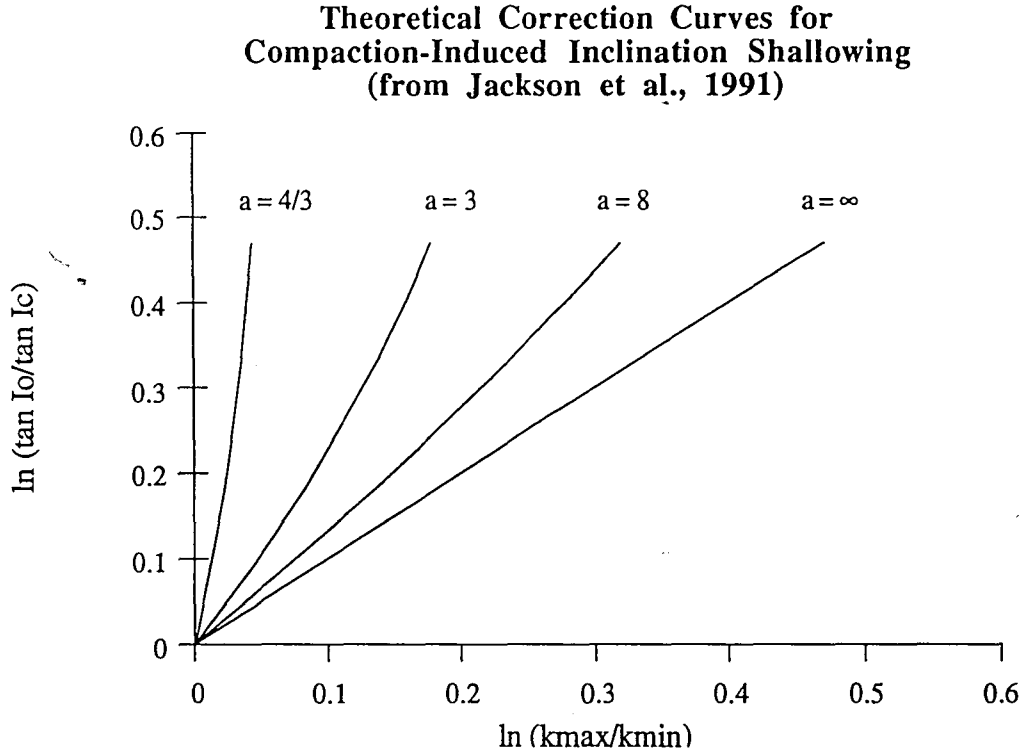

Figure 4
Theoretical correction curves for compaction-caused inclination shallowing. (From *Jackson et al., 1991*) Io and Ic are the expected and compacted inclinations, respectively. Kmax and kmin are the eigenvalues for the maximum and minimum directions of anisotropy, respectively. *a* is the particle anisotropy.

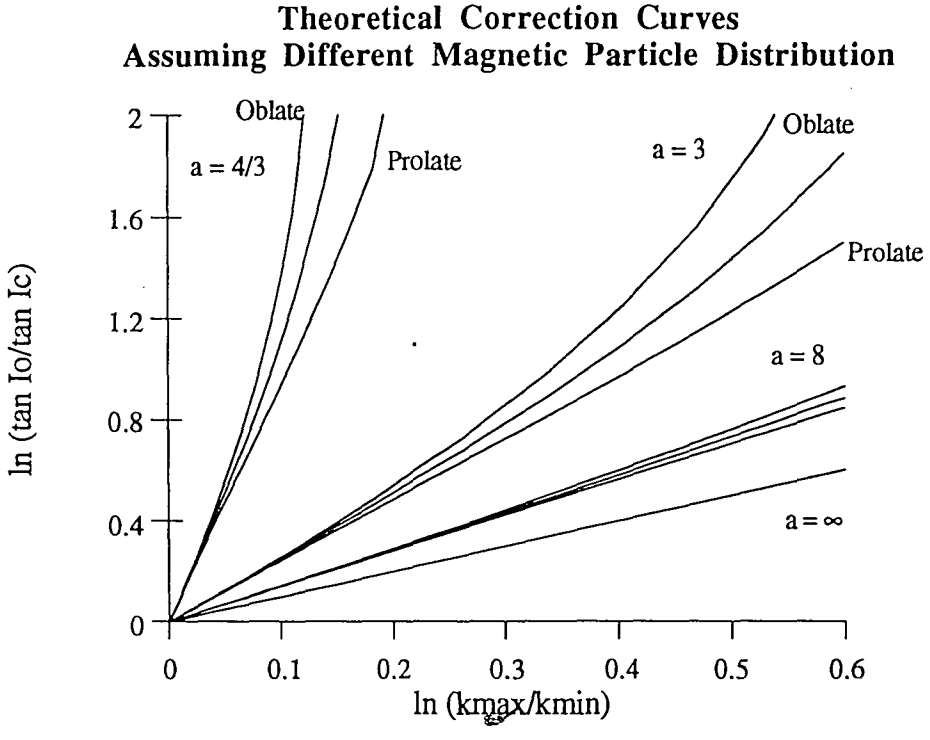

Figure 5
Theoretical inclination shallowing vs. anisotropy curve based on the model by *Jackson et al. (1991)* but assuming different magnetic particle distribution during compaction. The prolate curve assumes the y and z-directions of the deforming sample remain constant. The oblate curve assumes the x and y-directions of the sample remain constant during deformation (compaction). The middle curve assumes a triaxial magnetic particle distribution.

Results

Pigeon Point Formation

Rock Magnetic Results

Partial anhysteretic remanent magnetization (pARM) spectra reveal that the magnetic grains for the Pigeon Point Formation have coercivities which range from 20 mT to 70 mT (Fig. 6). This was the coercivity window used for the AAR measurements.

XRD Results

X-ray diffraction of the disaggregated sediments from the Pigeon Point Formation reveal high concentrations of quartz, kaolinite, and illite (Fig. 7). Therefore, the non-magnetic fraction of these rocks were assumed to consist of clay and silt matrix with a silica-rich cement. This assumption was confirmed by analyzing thin sections of core samples from the Pigeon Point Formation.

Paleomagnetic and AAR Results

The mean characteristic magnetization of thirteen samples from three sites in the Pigeon Point Formation collected in December 1991 is D=357.3°, I=56.6° with $\alpha(95)$=12.3°. Due to the small number of samples which yielded a characteristic magnetization (n=9) we augmented our data set with twenty-one samples from four sites provided by Duane Champion. The mean of the site means for the combined data set (n=7) is D=349.0°, I=43.4° with $\alpha(95)$=10.2° (Fig. 8). The combined data set agrees more closely to the mean direction published by *Champion et al. (1984)*

(D=320.1°, I=40.7° with $\alpha(95)=7.3°$). This was originally used as evidence to support the theory of large northward transport.

AAR measurements on the Pigeon Point samples show a fabric in which the maximum axes cluster about the N-S horizontal direction with the minimum axes forming a girdle perpendicular to it (Fig. 9).

Compaction Results

Although forty-two compaction experiments were performed, results from only six of these experiments were useful. The initial experimental results did not appear to have any change in inclination due to compaction. Upon further examination of the experimental procedure, it was found that the samples had acquired a viscous remanent magnetization (VRM). Removal of the VRM by AF demagnetization on six samples, after compaction, revealed that these samples did experience compaction shallowing. The inclination shallowing could not be monitored during the experiments, as previously done by other researchers *(Anson and Kodama, 1987; Deamer and Kodama, 1990; Kodama and Sun, 1991)*. These six samples allowed use of *Jackson et al.'s (1991)* model to correct for inclination shallowing.

Table 1

Compacted Pigeon Point Sediments

Sample	Magnetic Field Inclination	Initial Acquired Inclination	Compacted and AF Demagnetized Inclination	Maximum Pressure of Compaction (MPa)
325	52.4°	58.5°	43.5°	.0785
329	54.0°	61.4°	42.2°	.0785
401	53.0°	58.7°	49.4°	.1256
406	53.0°	59.6°	44.6°	.0314
412	54.2°	55.2°	41.7°	.0471
414	59.2°	64.9°	52.4°	.0628

Before compaction, the slurries were stirred to give them a post depositional remanence (pDRM). The inclination acquired by the sediments before compaction was from 1° to 6° steeper than the magnetic field in which the sediments were compacted. The difference between magnetic field inclination and the inclination acquired did not appear to change with continued stirring of the samples.

The results from the compacted Pigeon Point sediments are plotted with the theoretical curves derived from *Jackson et al. (1991)* (Fig. 11). The compacted Pigeon Point sediments lie close to the theoretical curve with a particle anisotropy of, a=4/3 . The compacted sediments do not have a perfect fit with the theoretical curve assuming either a prolate or an oblate magnetic particle distribution Due to the scatter of the data between the prolate and oblate magnetic particle distributions, a distinction between the two curves could not be made. Based on these results the AAR of the Pigeon Point samples can be used to correct their inclinations for compaction shallowing assuming a particle anisotropy of a=4/3.

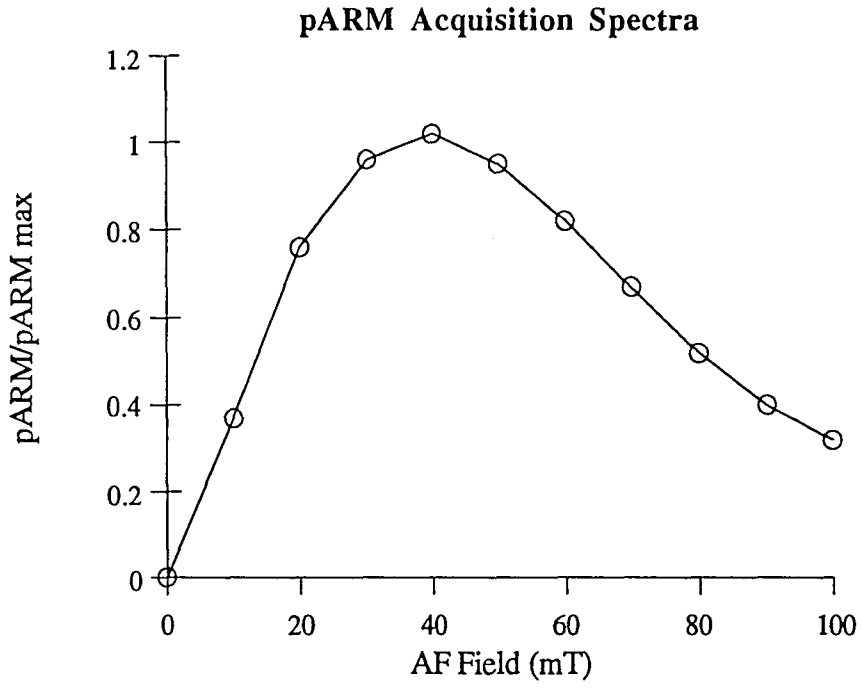

Figure 6
pARM acquisition spectrum of Pigeon Point Formation. The coercivity peak is centered at 40 mT. The spectrum indicates the presence of magnetite.

Figure 7
X-ray diffraction analysis of disaggregated Pigeon Point samples.
The analysis indicates large amounts of quartz with smaller amounts of illite and kaolinite. Y-axis is peak intensity in counts. X-axis is angle in degrees (2Θ).

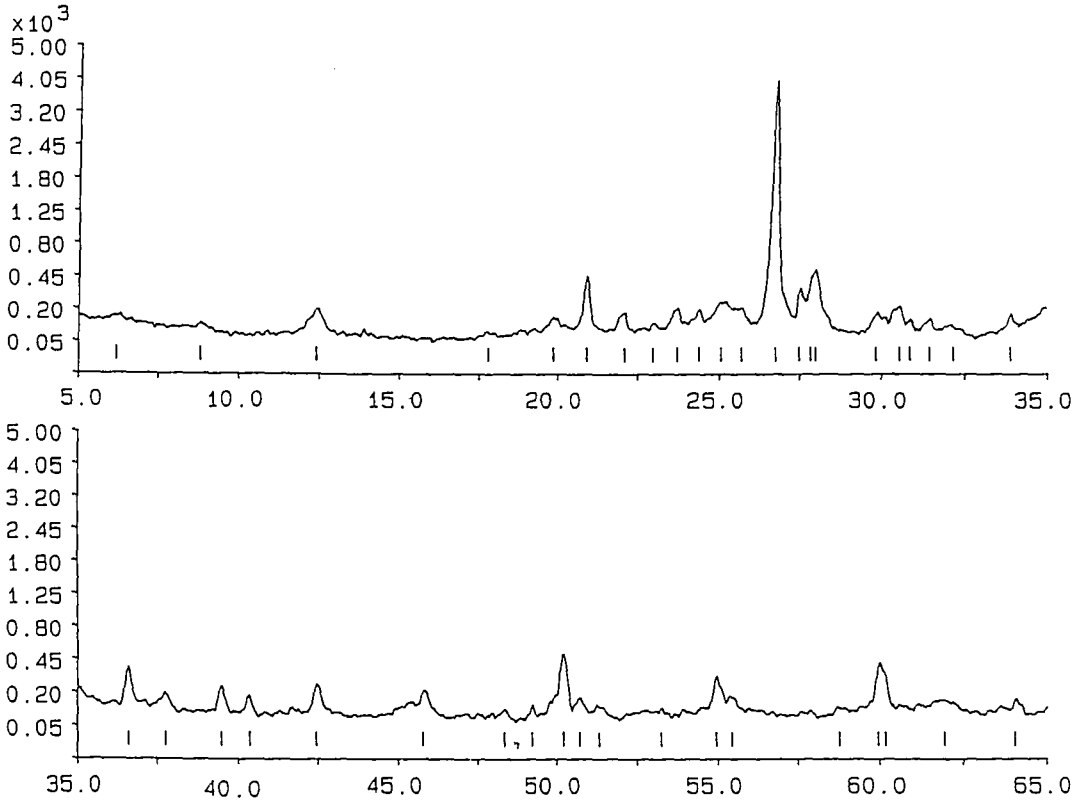
x10^3
5.00
4.05
3.20
2.45
1.80
1.25
0.80
0.45
0.20
0.05
5.0
10.0
15.0
20.0
25.0
30.0
35.0
5.00
4.05
3.20
2.45
1.80
1.25
0.80
0.45
0.20
0.05
35.0
40.0
45.0
50.0
55.0
60.0
65.0

Nacimiento Formation and Corral Quemado Formation

The results (Fig. 12) for the Nacimiento Formation and Corral Quemado Formation show that both units have points that lie between the theoretical curves with particle anisotropy a=4/3 and a=3. Neither the Nacimiento Formation nor the Corral Quemado Formation have a good fit to the *Jackson et al. (1991)* model. The data from the Nacimiento Formation are scattered between the a=4/3 and a=3 curves, with approximately one-half of the data lying near the a=4/3 curve and one-half of the data lying near the a=3 curve. The data from the Corral Quemado Formation show most of the data lying below the a=4/3 curve, with some data points lying directly on the a=4/3 curve. The most obvious feature of data sets from both the Nacimiento and Corral Quemado Formations is the large amount of scatter in the data.

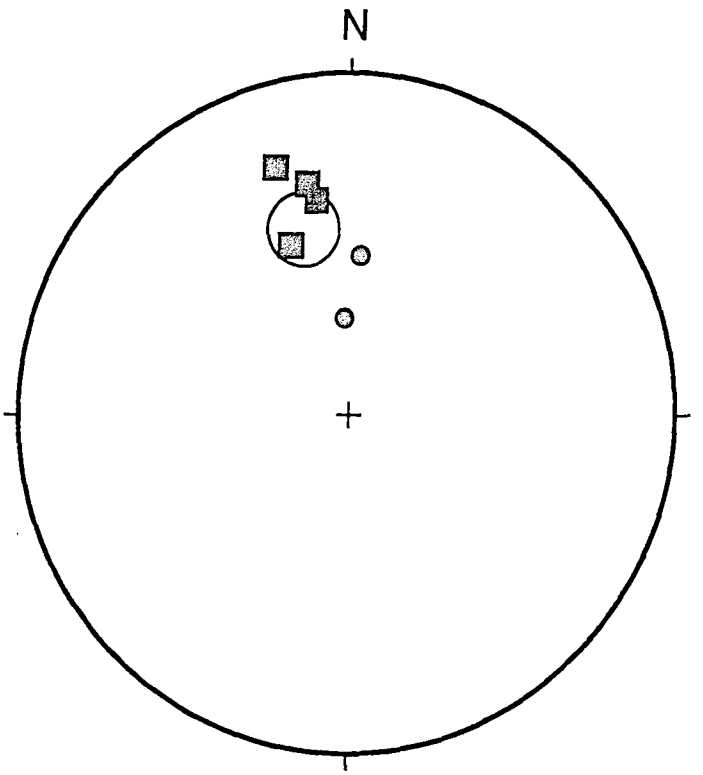

Pigeon Point
Site Means

Mean Inc = 43.36
Mean Dec = 348.95
Alpha 95 = 10.20

- Pigeon Point Sites-This Study
- Site from Champion et al., 1984

Figure 8
Equal-area stereographic projection of six site means from Pigeon Point. 95% confidence interval is represented by the circle.

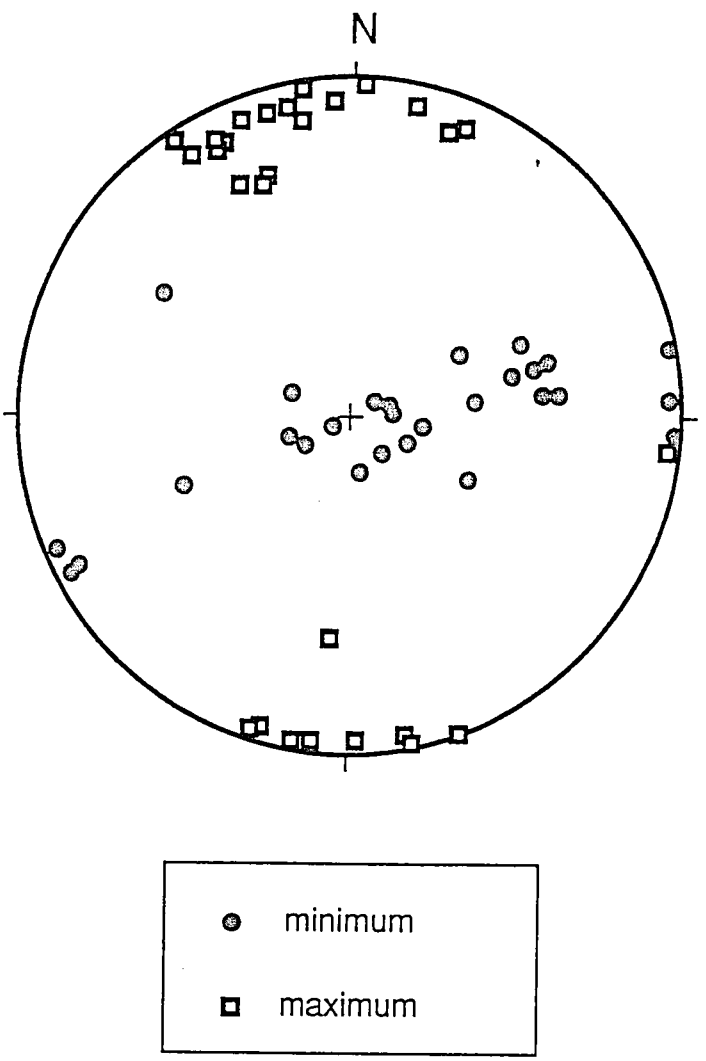

Figure 9
AAR of samples taken from the Pigeon Point Formation. The directions are plotted in stratigraphic coordinates. Minimum axes of anisotropy are plotted as circles. Maximum axes of anisotropy are plotted by squares.

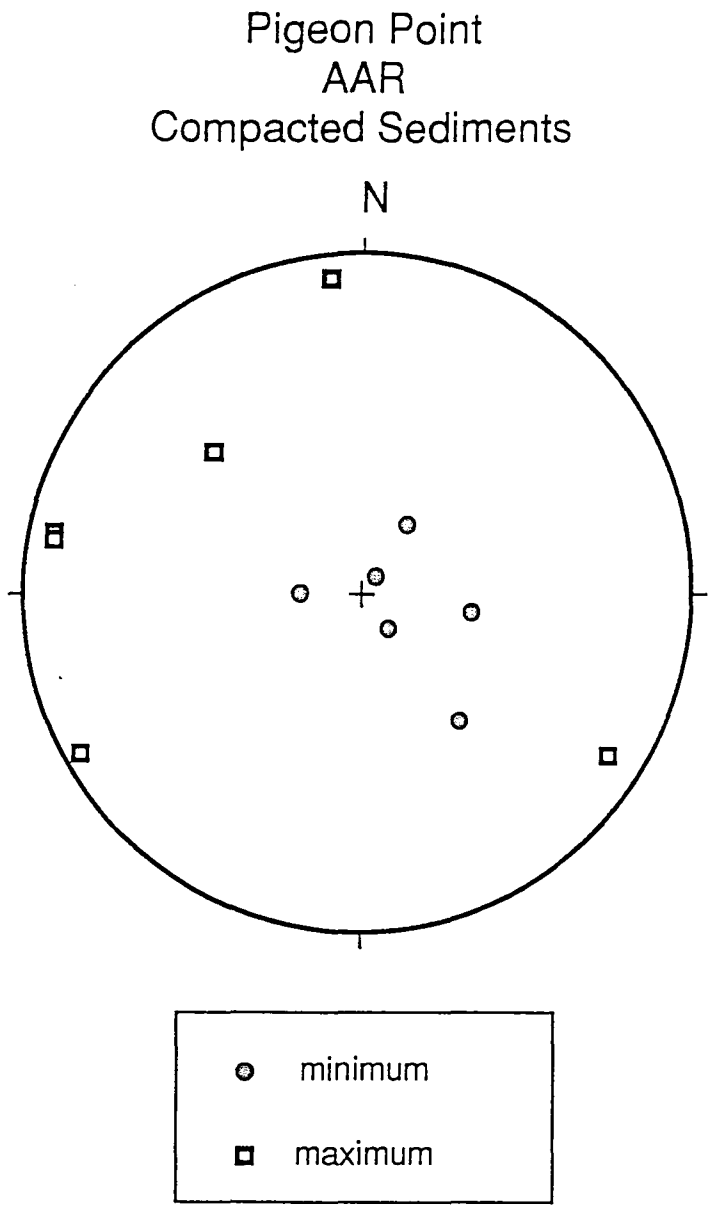

Figure 10
AAR of compacted Pigeon Point sediments. Minimum axes of anisotropy are plotted as circles. Maximum axes of anisotropy are plotted by squares.

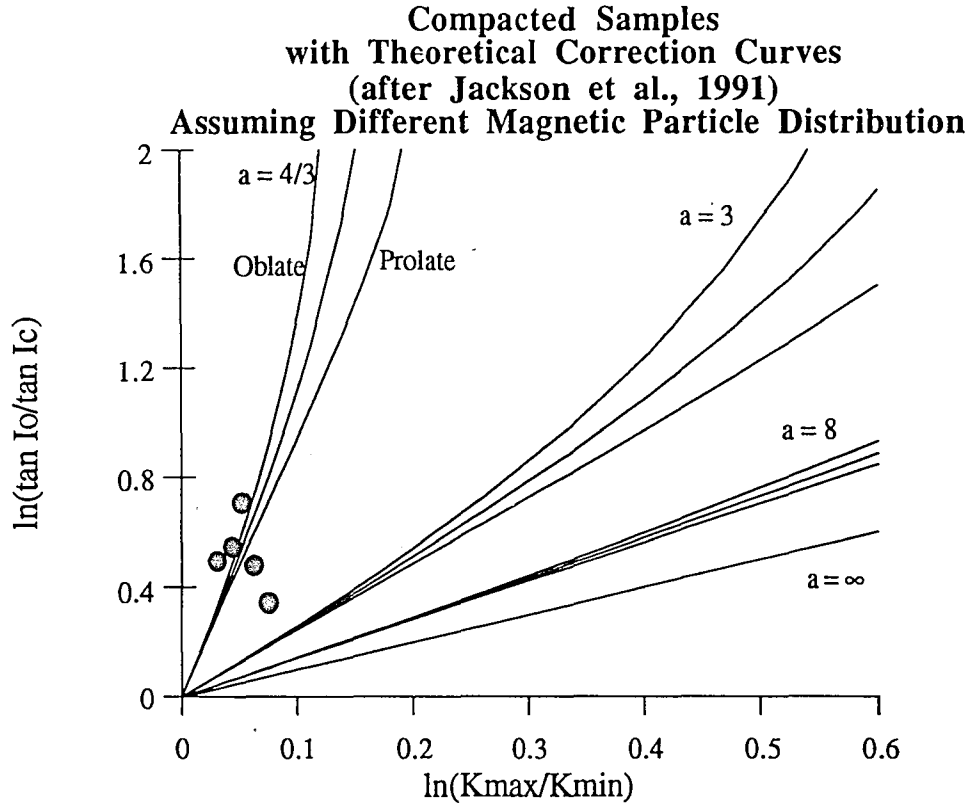

Figure 11
Inclination shallowing vs. anisotropy for compacted Pigeon Point sediments plotted with the theoretical correction curves derived from *Jackson et al. (1991)* based on the shape of the magnetic particle distribution.

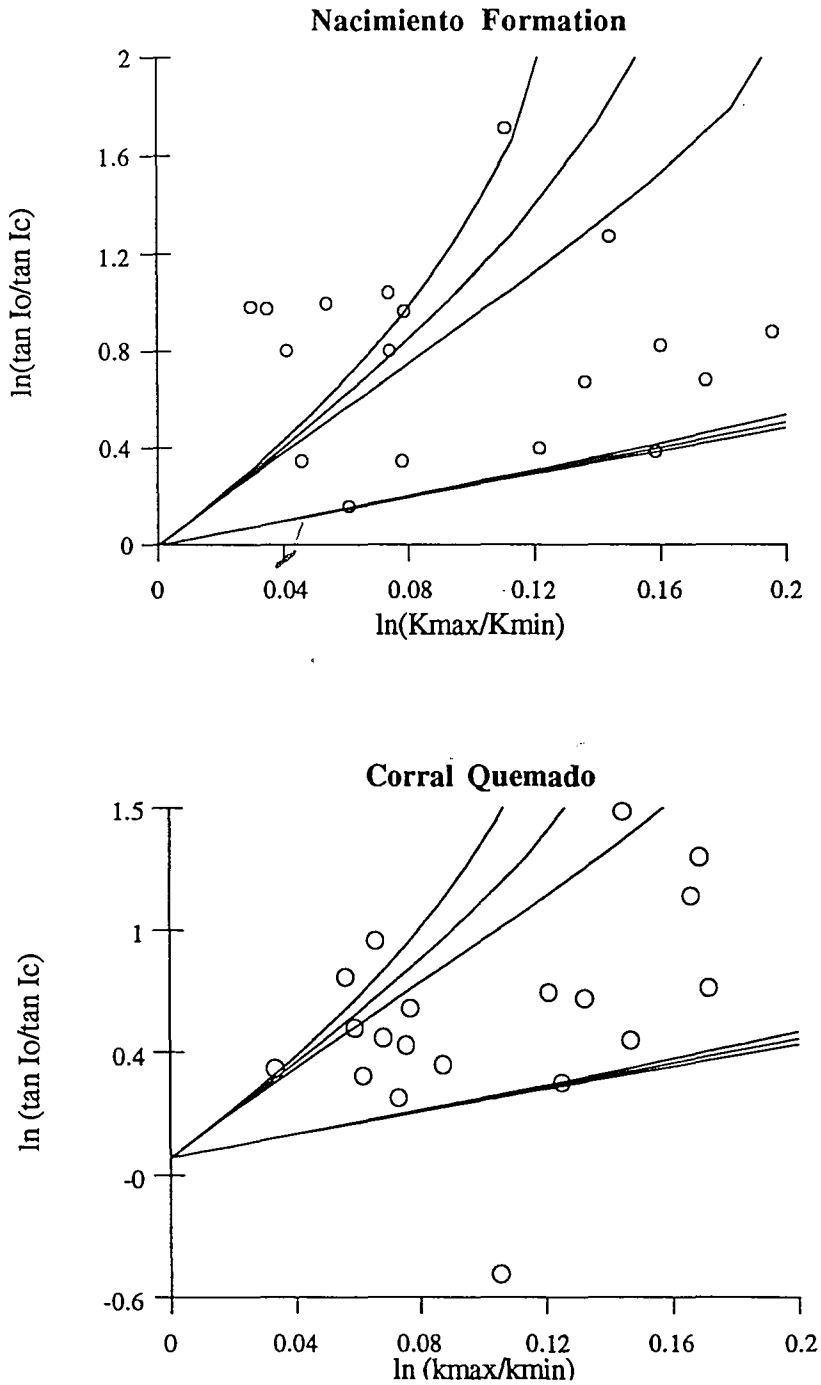

Figure 12
Inclination shallowing vs. anisotropy plotted for the Nacimiento Formation and Corral Quemado Formation against the theoretical correction curves derived from *Jackson et al. (1991)* but assuming different magnetic particle distribution during compaction.

Discussion

Compaction Data

The Pressure vs. Volume Loss curves (Fig. 3) all show a break in slope between pressures of 0.03 MPa and 0.07 MPa. In some cases, the plunger stuck after compaction had started. In general, all samples exhibit an initial rapid volume decrease from 0-0.03 MPa followed by lower rates of volume loss. This behavior is similar to previous experimental compaction work *(Anson and Kodama, 1987; Deamer and Kodama, 1990; Kodama and Sun, 1991)* on both synthetic and natural sediments. Total percent volume loss of the sediments after the abrupt change in slope ranged from 20-40%. These values are slightly lower than previous experimental work *(Anson and Kodama, 1987; Deamer and Kodama, 1990; Kodama and Sun, 1991)*. One possible explanation for the lower values is that this set of experiments used slurries with a water content of 100%, while previous experimental work used water content up to 200%.

Correction Curves

In order to use the theoretical curves to correct for inclination shallowing with anisotropy *(Jackson et al., 1991)* the individual magnetic grain particle anisotropy, *a* must be known. This parameter was not independently measured in this study. Instead, an estimation of *a* was made by fitting curves to the Inclination Shallowing vs. AAR results from the compaction experiments assuming the *Jackson et al. (1991)* model.

Once compaction experiments and AAR measurements were completed, a plot of $\ln(\tan I_O/\tan I_C)$ vs. $\ln(k_{max}/k_{min})$ was constructed. The data from this study do not agree completely with the theoretical curves of *Jackson et al. (1991)* (Fig. 4). *Jackson et al's. (1991)* curves, however, were generated assuming the development of

a triaxial magnetic particle distribution during compaction. The triaxial case has volume loss with one horizontal direction (y-direction) (See Appendix A) held constant. This type of deformation is not consistent with the lineated fabric observed in the Pigeon Point Formation samples (Fig. 9).

The AAR of the Pigeon Point samples shows the maximum axes cluster about a N-S horizontal direction with the minimum and intermediate axes forming a girdle perpendicular to it. This fabric probably results from high flow velocities during deposition of a turbidite. At the top of a turbidity flow, where finer sediments are deposited, the flow direction is perpendicular to the maximum axes. This creates a perpendicular-to-flow lineation due to traction transport*(Elwood et al., 1979)*. A compaction fabric would have then been imposed on this depositional fabric. Therefore, the Pigeon Point Formation has a composite fabric made up of a lineated, turbidity flow, depositional fabric and a foliated, compaction fabric.

To correct for inclination shallowing resulting from a lineated fabric, we generate a new set of correction curves based on the model by *Jackson et al (1991)*, assuming a prolate magnetic particle distribution in which the vertical direction (z-direction) and one horizontal direction (y-direction) are held constant during compaction. The prolate magnetic particle distribution correction curve is valid if the fabric in the Pigeon Point samples represents only the fabric resulting from the turbidity flow. Since the Pigeon Point samples probably have a composite fabric, which though dominated by the lineation probably also has effects of burial compaction, we also generate a new set of correction curves assuming an oblate magnetic particle distribution, where the two horizontal directions (x and y) are held constant. This fabric would result from a compaction. Correcting for the inclination shallowing caused by the composite fabric can be calculated using a theoretical correction curve derived from a combination of the prolate and oblate magnetic particle distributions (Fig. 5) instead. However, since we do not know the relative

contribution of each fabric, we will proceed by determining the compaction correction for both types of fabric. This will allow us to put bounds on our inclination shallowing correction.

Inherent in the assumption of a prolate ellipsoid for a lineated fabric (see Appendix C) is

$$q_X > q_Y = q_Z \tag{9}$$

Where q_X, q_Y, and q_Z represent k_{max}, k_{int} and k_{min}, respectively.

Since

$$q_X + q_Y + q_Z = 1 \tag{10}$$

Then from Equation (9)

$$\frac{q_X}{q_Y} = \text{ratio} = \frac{q_X}{q_Z} \tag{11}$$

Therefore the ratio of k_{max}:k_{int} is equal to k_{max}:k_{min} then Eqn. (8) can be written as

$$\ln\left(\frac{kmax}{\left(\frac{kmin + kint}{2}\right)}\right) = \ln\left(\frac{\tan(Io)}{\tan(Ic)}\right) \tag{12}$$

Similarly, the assumption for an oblate ellipsoid for a foliated fabric (see Appendix B) is

$$q_X = q_Y > q_Z \tag{13}$$

recalling

$$q_X + q_Y + q_Z = 1 \tag{11}$$

then

$$\frac{q_X}{q_Z} = \text{ratio} = \frac{q_Y}{q_Z} \tag{14}$$

And Eqn. (8) can be written as

$$\ln\left(\frac{\left(\frac{(kmax + kint)}{2}\right)}{(kmin)}\right) = \ln\left(\frac{\tan(Io)}{\tan(Ic)}\right) \qquad (15)$$

Equations (12) and (15) were invoked to correct for compaction-induced inclination shallowing for the Pigeon Point Formation for a particle anisotropy, a= 4/3, and assuming prolate and oblate magnetic particle distributions, respectively (Tables 2 and 3).

The 'corrected' mean of the site means, assuming a lineated fabric for the Pigeon Point Formation is D= 351.6°, I= 53.1° with $\alpha(95)$= 11.3°, and assuming a foliated fabric it is D= 349.4°, I= 50.4° with $\alpha(95)$= 10.4° (Table 4) (Fig. 13) The inclination of the mean of the site means originally reported by *Champion et al. (1984)*, in support of the large northward transport theory, is 40.7°. The corrected inclinations calculated here are 10°-13° steeper than those reported by *Champion et al. (1984)*, but are still shallow compared to the expected Cretaceous inclination value of 66° for the Pigeon Point Formation.

Tectonic Implications

A new paleolatitude for the Pigeon Point Formation has been calculated (Table 4) that differs from the paleolatitude previously reported by *Champion et al. (1984)* by approximately 10°. The new paleolatitude predicts 1400 km to 1700 km of northward transport of the Pigeon Point Formation, with respect to the Late Cretaceous pole for cratonic North America.

Determination of displacements along local fault systems, the San Andreas and San Gregorio, can account for some the offset. Estimates of displacements on the San Andreas fault, based on molluscan faunal patterns and stratigraphic correlations, suggest 305 km of right-lateral displacement since early Miocene time *(Champion et*

al., 1984). Estimates of displacement of the San Gregorio fault system suggest a minimum of 90 km of right-lateral motion since Miocene time *(Mullins and Nagal, 1981; Graham and Dickinson, 1978).* Considering these fault systems can only accommodate about 400 km of the offset, we still need to account for 1000 km to 1200 km.

Once compaction-induced inclination shallowing is taken into account, (Fig. 14) it is apparent that the previous pattern of apparent latitudinal transport of the Santa Lucia allochthon (SLOA), which showed a linear decrease from 90 Ma to 55 Ma, is no longer accurate. The Pigeon Point Formation paleolatitude is now consistent with nearly all other SLOA and Baja-Borderland allochthon (BBA) paleolatitudes at approximately 75 Ma. The exception to this grouping is the Fish Creek Turbidites *(McWilliams and Howell, 1982)* . This grouping of data indicates approximately 15° of apparent latitudinal transport and would suggest that the BBA and SLOA were not two separate terranes but that they both experienced transport as one system. Treating the SLOA and BBA as one system can reduce the need for complex motion histories needed to explain the more southerly latitudes of SLOA as previously interpreted *(Butler et al., 1991).* This interpretation also suggests that the results from the Cretaceous age Fish Creek Turbidites *(McWilliams and Howell, 1982)* should be examined for possible compaction shallowing.

Table 2

Pigeon Point Samples Corrected for Inclination Shallowing

Assuming a Prolate Magnetic Particle Distribution with $a = 1.33$

Sample	ln (k_{max}/k_{avg}*)	ln (1/f)	Compacted Inclination (°)	Corrected Inclination (°)	Corrected Declination (°)
PP1	0.037826	0.406	46.6	56.6	39.6
PP2-2			43.1		
PP3	0.054744	0.614	42.8	57.2	25.8
PP3-2			66.6		
PP8	0.070957	0.839	28.1	46.0	320.6
PP16-2	0.037267	0.399	39.2	49.3	355.00
PP17	0.094674	1.240	52.6	72.4	11.0
PP19-2			86.3		
PP21-2	0.063440	0.731	75.3	81.8	283.8
1-1	0.056853	0.642	12.1	20.1	346.5
2-1	0.046743	0.513	38.2	50.8	327.0
3-1	0.043905	0.478	14.8	21.9	328.3
4-1	0.066097	0.769	27.6	44.2	4.2
5-1	0.080413	0.986	54.7	71.5	334.9
6-1	0.077799	0.944	32.2	52.5	328.4
7-1	0.081628	1.006	59.9	74.9	355.1
8-1	0.077294	0.936	7.6	15.4	349.5
9-1	0.095555	1.258	5.6	13.4	7.0
11-2	0.070071	0.826	22.9	39.1	341.2
12-1	0.080747	0.992	65.2	77.7	318.8
13-1	0.066454	0.774	36.3	53.9	336.5
15-1	0.051425	0.571	73.6	79.7	28.8
16-1	0.080483	0.987	22.7	41.6	346.3
17-2	0.040148	0.433	38.4	49.3	348.5
19-1	0.102330	1.398	67.3	80.8	304.2
22-1	0.048022	0.529	34.9	47.7	338.1
23-1	0.050012	0.554	37.6	51.0	350.0
24-1	0.063459	0.731	29.9	46.2	351.5
25-2	0.050348	0.558	23.2	34.6	346.0
26-1	0.061255	0.701	32.9	49.0	355.8

*where $k_{avg}=[(k_{min} + k_{int})/2]$
Samples with prefix PP are samples collected for this study, all other samples are from *Champion et al.'s (1984)* study

Table 3

Pigeon Point Samples Corrected for Inclination Shallowing
Assuming an Oblate Magnetic Particle Distribution with $a = 1.33$

Sample	ln (k_{avg}*/k_{min})	ln (1/f)	Compacted Inclination (°)	Corrected Inclination (°)	Corrected Declination (°)
PP1	0.061189	0.700	46.6	64.8	39.6
PP2-2			43.1		
PP3	0.061001	0.698	42.8	61.7	25.8
PP3-2			66.6		
PP8	0.049932	0.553	28.1	42.9	320.6
PP16-2	0.046311	0.508	39.2	53.6	355.00
PP17	0.040850	0.441	52.6	63.8	11.0
PP19-2			86.3		
PP21-2	0.049932	0.553	75.3	81.4	283.8
1-1	0.036332	0.388	12.1	17.5	346.5
2-1	0.034694	0.369	38.2	48.7	327.0
3-1	0.033452	0.355	14.8	20.6	328.3
4-1	0.047785	0.526	27.6	41.5	4.2
5-1	0.054327	0.609	54.7	68.9	334.9
6-1	0.053296	0.595	32.2	48.8	328.4
7-1	0.049811	0.551	59.9	71.5	355.1
8-1	0.062351	0.716	7.6	15.3	349.5
9-1	0.061870	0.709	5.6	11.3	7.0
11-2	0.041306	0.447	22.9	33.4	341.2
12-1	0.053801	0.602	65.2	75.8	318.8
13-1	0.043472	0.473	36.3	49.7	336.5
15-1	0.036393	0.389	73.6	78.7	28.8
16-1	0.050345	0.558	22.7	36.2	346.3
17-2	0.032067	0.339	38.4	48.1	348.5
19-1	0.055025	0.618	67.3	77.3	304.2
22-1	0.041969	0.455	34.9	47.7	338.1
23-1	0.050157	0.555	37.6	53.3	350.0
24-1	0.039068	0.420	29.9	41.2	351.5
25-2	0.035683	0.381	23.2	32.1	346.0
26-1	0.050358	0.558	32.9	48.5	355.8

*where $k_{avg}=[(k_{max} + k_{int})/2]$
Samples with prefix PP are samples collected for this study, all other samples are from *Champion et al.'s (1984)* study

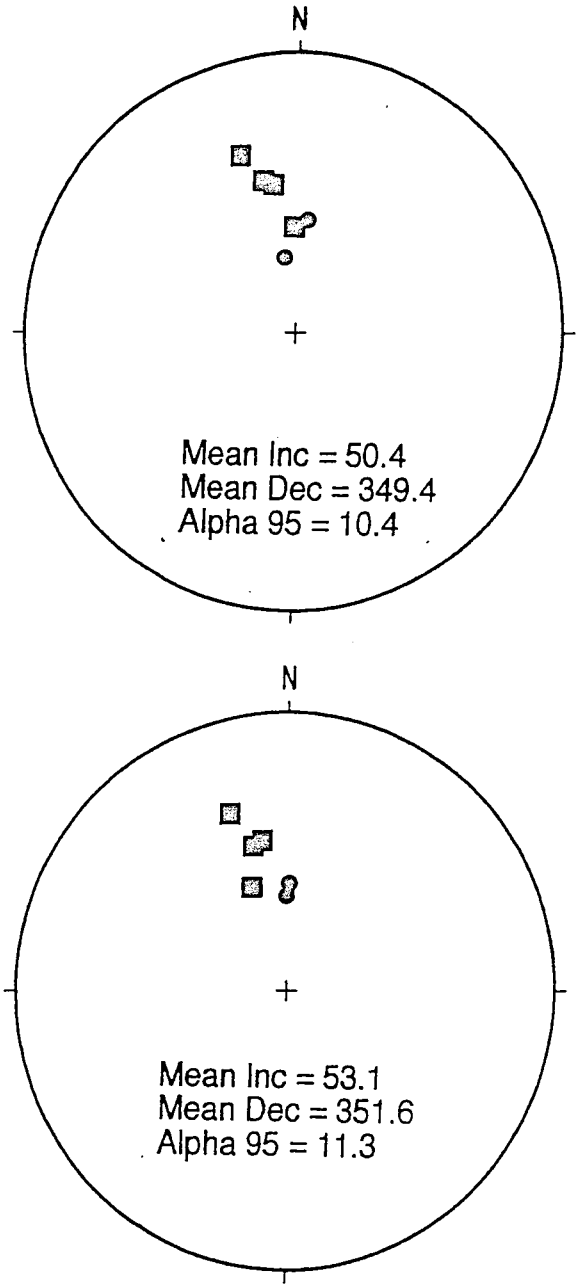

Figure 13
Equal-area stereographic projection of six site means from Pigeon Point corrected for inclination shallowing assuming different magnetic particle distributions.

Table 4
Predicted Paleolatitude, Paleomagnetic Field Directions, Latitudinal Offset and Total Offset of Pigeon Point from Different Studies

Reference	Paleolatitude (°N)	Inclination (°)	Declination (°)	Latitudinal Offset (°)	Total Offset (km)
Expected Cretaceous Pole	46.5	64.6	333.3	*	*
Champion et al. (1984)	23.2	40.7	320.1	23.2	2578
This Study uncorrected for inclination shallowing	25.3	43.4	349.0	21.2	2353
This Study corrected assuming prolate sample	33.6	53.1	351.6	12.8	1420
This Study corrected assuming oblate sample	31.1	50.4	349.4	15.4	1709

Nacimiento and Corral Quemado Formations

It is obvious from the results in Fig. 12 that there are other factors, besides magnetic particle anisotropy, controlling inclination shallowing. The results for the Corral Quemado Formation scatter around the ln(kmax/kmin) axis, which would indicates no inclination shallowing, although there is still some scatter. The results from the Nacimiento Formation have such a large amount of scatter that there does not seem to be any preference for the data toward the a=4/3 curve, which would be expected for a known inclination shallowing.

One explanation for these results could be related to the clay content and magnetic mineral grain sizes of both formations. If there is a range of magnetic grain

sizes, with a range of grain anisotropy, there would be a large scatter on the inclination shallowing vs. anisotropy curves.

To better understand the results from the Nacimiento and Corral Quemado Formations a detailed rock magnetic study along with experimental compaction work needs to be done. The compaction experiments can confirm the results seen in Fig. 12, while the rock magnetic study can determine the magnetic grain particle anisotropies.

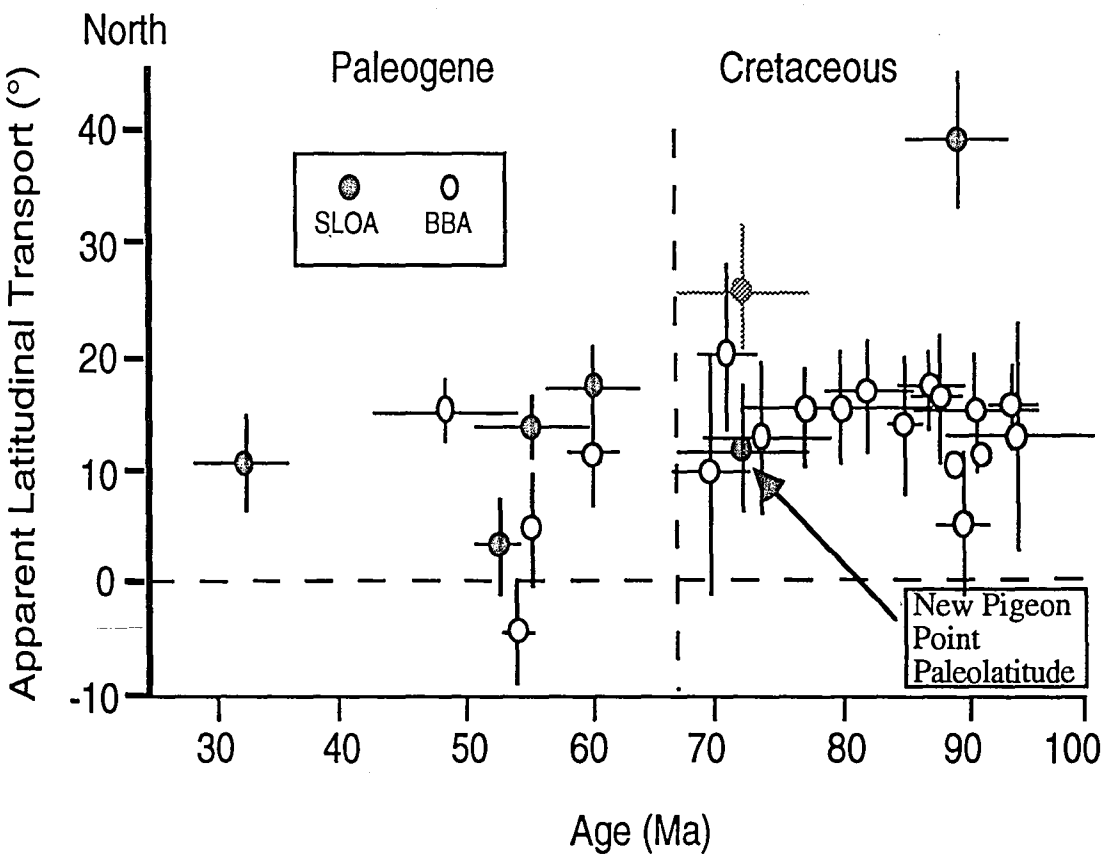

Figure 14
Apparent northward transport determined from Cretaceous and Paleogene sedimentary rocks of the Santa Lucia Orocopia (SLOA) and Baja-Borderland allochthon (BBA) versus age of geologic unit. Stippled data point is Pigeon Point paleolatitude predicted by *Champion et al. (1984)*. New Pigeon Point paleolatitude determined by correcting for compaction-induced inclination shallowing is indicated by arrow. Vertical error bars are 95% confidence on latitudinal transport. Range of age is indicated by horizontal bar through each data point. (From *Butler et al., 1991*)

Conclusions

1. The Pigeon Point Formation has a composite fabric, from compaction and turbidity flow deposition, which has resulted in a shallowed inclination.

2. The shallowed inclinations of the Pigeon Point Formation have been corrected using the model by Jackson et al. (1991) along with experimental compaction studies on Pigeon Point sediments.

3. Based on corrections for compaction-induced inclination shallowing, the Pigeon Point Formation has experienced approximately 1500 km of northward transport, not 2500 km as previously reported by *Champion et al. (1984).* This amount of offset brings the Santa Lucia-Orocopia allochthon (SLOA) in agreement with the offsets of the Baja-Borderland allochthon (BBA) at 72 Ma.

4. There needs to be more detailed rock magnetic and compaction studies work on the Nacimiento and Corral Quemado Formations in order to better understand the results seen in this study.

Appendix A
Triaxial Magnetic Particle Distribution

Assuming $q_x > q_y > q_z$

for a volume loss with one horizontal dimension held constant.

Where $q_x + q_y + q_z = 1$ and $\frac{q_x}{q_y} = \text{ratio}$

assume $q_y = \frac{1}{3}$

So $$q_x = \frac{\frac{2}{3}}{\left(1 + \frac{1}{\text{ratio}}\right)}$$

and $$q_z = \frac{\frac{2}{3}}{(1 + \text{ratio})}$$

So $$\frac{1}{f} = \frac{\left(\left(\frac{\left(\frac{2}{3}\right)}{1 + \frac{1}{\text{ratio}}}\right)(a+2) - 1\right)}{\left(\left(\frac{\left(\frac{2}{3}\right)}{1 + \text{ratio}}\right)(a+2) - 1\right)}$$

Appendix B
Oblate Magnetic Particle Distribution

Assuming $q_x = q_y > q_z$
an oblate ellipsoid for a foliated fabric.
Where $q_x + q_y + q_z = 1$

and $\frac{q_x}{q_z} = \text{ratio} = \frac{q_y}{q_z}$

for q_x

1) $2q_x = 1 - q_z$

2) $q_z = \frac{q_x}{\text{ratio}}$

3) $2q_x = 1 - \frac{q_x}{\text{ratio}}$

4) $2q_x + \frac{q_x}{\text{ratio}} = 1$

5) $q_x\left(2 + \frac{1}{\text{ratio}}\right) = 1$

therefore 6) $q_x = \frac{1}{2 + \frac{1}{\text{ratio}}}$

for q_z

1) $q_z + 2q_x = 1$

2) $q_x = \frac{q_z}{\text{ratio}}$

3) $q_z + 2(q_z * \text{ratio}) = 1$

4) $q_z\,(1 + 2*\text{ratio}) = 1$

therefore 5) $q_z = \frac{1}{1 + 2*\text{ratio}}$

So $$\frac{1}{f} = \left(\frac{\left(\frac{1}{\left(2 + \frac{1}{\text{ratio}}\right)}\right)(a+2) - 1}{\left(\frac{1}{1 + 2 * \text{ratio}}\right)(a+2) - 1} \right)$$

Appendix C
Prolate Magnetic Particle Distribution

Assuming $q_x > q_y = q_z$

a prolate ellipsoid for a lineated fabric.

Where $q_x + q_y + q_z = 1$

and $\frac{q_x}{q_y} = \text{ratio} = \frac{q_x}{q_z}$

Then for q_x

1) $q_x + 2q_y = 1$

2) $q_y = \frac{q_x}{\text{ratio}}$

So 3) $q_x = 1 - 2\left(\frac{q_x}{\text{ratio}}\right)$

4) $q_x + 2\left(\frac{q_x}{\text{ratio}}\right) = 1$

5) $q_x\left(1 + \frac{2}{\text{ratio}}\right) = 1$

therefore $q_x = \frac{1}{\left(1 + \frac{2}{\text{ratio}}\right)}$

for q_y

1) $2q_y = 1 - q_x$

but 2) $q_x = \text{ratio} * q_y$

So : 3) $2q_y = 1 - \text{ratio} * q_y$

4) $q_y(2 + \text{ratio}) = 1$

therefore: $q_y = \frac{1}{2 + \text{ratio}}$

and $\frac{1}{f} = \left(\frac{\left(\left(\frac{1}{\left(1 + \frac{2}{\text{ratio}}\right)}\right)(a + 2) - 1\right)}{\left(\frac{1}{2 + \text{ratio}}\right)(a + 2) - 1}\right)$

References

Anson, G.L. and K.P. Kodama, Compaction induced inclination shallowing of the post-depositional remanent magnetization in a synthetic sediment, *Geophysical Journal of the Royal Astronomical Society*, 88, 673-692, 1987.

Arason, G.L. and S. Levi, Compaction and inclination shallowing in deepsea sediments from the Pacific Ocean, *Journal of Geophysical Research*, 95, 4501-4510, 1990.

Arason, P. and S. Levi, Inclination shallowing recorded in some deep sea sediments, *EOS Trans. AGU*, 916, 1986.

Barton, R.H. and M.W. McElhinny, Detrital remanent magnetization in five slowly deposited long cores of sediment, *Geophysical Research Letters*, 6, 232-292, 1979.

Blow, R.A. and N. Hamilton, Effects of compaction on the acquisition of a detrital remanent magnetism in fine grained sediments, *Geophysical Journal of the Royal Astronomical Society*, 52, 13-23, 1978.

Butler, R.F., W.R. Dickinson and G.E. Gehrels, Paleomagnetism of coastal California and Baja California: Alternatives to large-scale northward transport, *Tectonics*, 10, 561-576, 1991.

Butler, R.F., L.G. Marshall, R.E. Drake and G.H. Curtis, Magnetic polarity stratigraphy and ^{40}K-^{40}AR dating of late Miocene and early Pliocene continental deposits, Catamarca Province, NW Argentina., *Journal of Geology*, 92, 623-636, 1984.

Butler, R.F. and L.H. Taylor, A middle Paleocene paleomagnetic pole from the Nacimiento Formation., *Geology*, 6, 495-498, 1978.

Celaya, M.A. and B.M. Clement, Inclination shallowing from deep-sea sediments from the North Atlantic, *Geophysical Research Letters*, 15, 52-55, 1988.

Champion, D.E., D.G. Howell and C.S. Gromme, Paleomagnetic and geologic data indicating 2500km of northward displacement for the Salinian and related terranes, California, *Journal of Geophysical Research*, 89, 7736-7752, 1984.

Deamer, G.A. and K.P. Kodama, Compaction induced inclination shallowing in synthetic and natural clay rich sediments, *Journal of Geophysical Research*, 95, 4511-4529, 1990.

Diehl, J.F., M.E. Beck, S. Beske-Diehl, D. Jacobson and B.C.H. Jr., Paleomagnetism of the Late Cretaceous-Early Tertiary North-Central Montana Alkalic Province, *Journal of Geophysical Research*, 88, 10593-10609, 1983.

Ellwood, B.B., Bioturbation: Minimal effects on the magnetic fabric of some natural and experimental sediments, *Earth and Planetary Science Letters*, 67, 367-376, 1984.

Graham, S.A. and W.R. Dickinson, Apparent offsets of on-land geologic features across the San Gregorio-Hosgri fault trend, *Spec. Rep. Calif. Div. Mines Geol.*, 137, 13-23, 1978.

Hagstrum, J.T., M. McWilliams, D.G. Howell and S. Grommé, Mesozoic paleomagnetism and northward translation of the Baja California Peninsula, Mexico, *Geological Society of America Bulletin*, 96, 1077-1090, 1985.

Hamano, Y., An experiment on the post-depositional remanent magnetization in artificial and natural sediments, *Earth and Planetary Science Letters*, 51, 221-232, 1980.

Howell, D.G. and J.G. Vedder, Late Cretaceous paleogeography of the Salinian Block, California, in *Mesozoic Paleogeography of the Western United States*, vol. edited by D.G. Howell and K.A. McDougall, pp. 523-534, Pacific Section, Society of Economic Paleontologists and Mineralogists, Los Angeles, 1978.

Irving, E., Origin of the paleomagnetism of the Torridonian sandstones of north-west Scotland, *Philos. Trans. R. Soc. London Ser. A*, 250, 100-110, 1957.

Irving, E. and A. Major, Post-depositional detrital remanent magnetization in a synthetic sediment, *Sedimentology*, 3, 135-143, 1964.

Jackson, M., Anisotropy of magnetic remanence: A brief overview of mineralogical sources, physical origins, and geological applications, and comparison with susceptibility anisotropy, *PaleoGeophysics*, 136, 1-29, 1991.

Kanter, L.R., Paleolatitude of the Butano Sandstone, California, and its implications for the kinematic histories of the Salinian terrane and the San Andreas Fault, *Journal of Geophysical Research*, 93, 11699-11710, 1988.

Kanter, L.R. and M. Debiche, Modeling the motion histories of the Point Arena and central Salinian terranes, in *Tectonostratigraphic Terranes of the Circum-Pacific Region: Houston Circum-Pacific Council for Energy and Mineral Resource Services*, vol. 1, edited by D.G. Howell, pp. 85-108, American Association of Petroleum Geologists, Tulsa, 1985.

Kent, D.V., Post depositional remanent magnetization in deep-sea sediment., *Nature*, 246, 32-34, 1973.

King, R.F., Depositional remanent magnetization in sediments, *Mon. Notic. Royal Astronomical Society*, 7, 115-134, 1955.

Kirschvink, J.L., The least-squares line and plane and the analysis of paleomagnetic data, *Geophysical Journal of the Royal Astronomical Society*, 62, 699-718, 1980.

Kodama, K.P., Remanence rotation due to rock strain during folding and the stepwise application of the fold test, *Journal of Geophysical Research*, 93, 3357-3371, 1988.

Kodama, K.P., Depositional Remanent Magnetization, in *Encyclopedia of Earth System Science*, vol. 2, edited by pp. 47-54, Academic Press, 1992.

Kodama, K.P. and A.G. Goldstein, Experimantal simple shear deformation of magnetic remanence, *Earth and Planetary Science Letters*, 104, 80-88, 1991.

Kodama, K.P. and W.W. Sun, Magnetic anisotropy as a correction for compaction-casued paleomagnetic inclination shallowing, *Geophysical Journal International*, 1992.

Levi, S. and S.K. Banerjee, On the origin of inclination shallowing in redeposited sediments, *Journal of Geophysical Research*, 95, 4383-4389, 1990.

McCabe, C., M.C. Jackson and B.B. Ellwood, Magnetic anisotropy in the Trenton limestone: results of a new technique, anisotropy of anhysteretic suscetibility and remanence in minerals, *Geophysical Research Letters*, 15, 333-336, 1985.

Mullins, H.T. and D.K. Nagal, Franciscan-type rocks off Monterey Bay, California: Implications for western boundary of Salinian block, *Geo. Mar. Lett.*, 1, 135-139, 1981.

Opdyke, N.D. and K.W. Henry, A test of the dipole hypothesis, *Earth and Planetary Science Letters*, 6, 138-151, 1969.

Patterson, D.L., Paleomagnetism of the Valle Formation and Late Cretaceous paleogeography of the Vizcaino Basin, Baja California, Mexico, in *Geology of the Baja California Peninsula*, vol. edited by V.A. Frizzell, pp. Pacific Section, Society of Economic Paleontologists and Mineralogists, Los Angeles, 1984.

Silver, L.T. and B.W. Chappell, The Peninsular Ranges Batholith: An insight into the evolution of the Cordilleran batholiths of southwestern North America, *Trans. Royal Soc. Edinburgh Earth Sci.*, 79, 105-121, 1988.

Silver, L.T., H.P. Taylor and B.W. Chappell, Some petrological, geochemical and geochronological observations of the Peninsular Ranges Batholith near the international border of the U.S.A. and Mexico, in *Mesozoic Crystalline Rocks: Peninsular Ranges Batholith and Pegmatites and Point Sal Ophiolite*, vol. edited by P.L. Abbott and V.L. Todd, pp. 83-110, Dept. of Geological Sciences, San Diego State University, San Diego, California, 1979.

Simpson, R.W. and A. Cox, Paleomagnetic evidence for tectonic rotation of the Oregon Coast Range, *Geology*, 5, 585-589, 1977.

Tarduno, J.A., Absolute inclination values from deep sea sediments: A reexamination of the Cretaceous Pacific record, *Geophysical Research Letters*, 17, 101-104, 1990.

Teissere, R.F. and M.E. Beck, Divergent Cretaceous paleomagnetic pole position for the Southern California Batholith, U. S. A., *Earth and Planetary Science Letters*, 18, 296-300, 1973.

Tucker, P., Stirred remanent magnetization: A laboratory analogue of post-depositional realignment, *Journal of Geophysics*, 48, 153-157, 1980.

Verosub, K.L., Depositional and post-depositional processes in the magnetization of sediments, *Reviews of Geophysics and Space Geophysics*, 15, 129-143, 1977.

Vita

Jodie Davi was born in Pleasantville, New York in 1968. She was raised in Pleasantville and graduated from Westlake High School in 1986. SHe received her B.S. from S. U. N. Y. Albany in 1990. She began attending Lehigh University in the Fall semester of 1991 to pursue a master's degree. She received her M.S. in December 1993.

END

OF

TITLE